

Development of Cu substituted Ni-Zn nano-ferrites for industrial applications

NAMAHARI KUMAR and DACHEPALLI RAVINDER*,
Department of Physics, Osmania University, Hyderabad- 50007, Telangana, India.

ABSTRACT

Cu substituted Nickel-Zinc ferrite nano-particles with composition $\text{Ni}_{0.2}\text{Cu}_x\text{Zn}_{0.8-x}\text{Fe}_2\text{O}_4$ ($x=0.0$ to 0.8 with step size 0.2) were synthesized using the technique of Citrate-Gel Auto Combustion method at 180°C . Sintering of prepared samples at 500°C for four hours was done and analyzed with XRD. These samples were confirmed with spinel structure of single phase. Size of the crystal, density of x-ray, volume and lattice parameter are being computed from XRD data. These nano-particles show UV-Vis absorption band in the wavelength region between 200 nm to 800 nm . High temperature thermo electrical Power studies have been carried out starting from room temperature to a temperature well beyond Curie temperature by differential method. Depending on the sign of Seebeck coefficient current nano-ferrites under study are classified as P-type semiconductors. All composition of Ni-Zn-Cu nano-ferrites are useful in Semi conductor industry. Electrical conductivity of Ni-Zn -Cu nano-ferrites have been studied by two probe method. The electrical conduction in these nano-ferrites is explained on the basis of hopping mechanism. The activation energy in the ferrimagnetic region is in general less than that in paramagnetic region.

KEYWORDS: Nano-ferrites; XRD; UV Spectroscopy; Thermo Electric Power; Electrical Conductivity;

Date of Submission: 10-09-2021

Date of Acceptance: 24-09-2021

I. INTRODUCTION

The magnetic behavior of materials can be classified into different types given by dia, para, ferro, ferric and anti-ferromagnetic materials. Among these ferrites magnetic properties of extraordinary range are exhibited by huge class of oxides. The magnetic lines of force in a ferromagnetic material are due to the applied magnetic field. In these materials magnetic susceptibility is large, positive and decreases with increase in temperature as per Curie-Weiss law. Ferromagnetism is supported by electron spin and the material acts as a powerful magnet. They are widely used in industry and devices like electric motors, generators, transformers, telephone, loudspeakers, magnetic stripe in credit cards. The main advantage of ferrites is its compositional variability of very high degree. Nano-particle ferrites play significant role in view of their extensive applications. Their physical and chemical properties remarkably differ from their bulk counterparts making them highly potential for different technical applications. Grain boundaries control their transport properties instead of grain itself [1]. Different chemical methods can be used to obtain high level molecular mixing, chemical homogeneity etc. while synthesizing spinel ferrites [2-5]. Synthesis of

Nickel-Copper -Zinc ferrites using ceramic, refluxing, combustion, hydrothermal, reverse micelle, co-precipitation, micro emulsion, ball milling and spark plasma sintering methods were already reported [6-13].

The present work reports some of the results obtained related to synthesized Ni-Cu-Zn ferrites such as XRD analysis, UV spectroscopy, Temperature dependence of electrical conductivity, Thermo Electric Power and Magnetic properties.

II. EXPERIMENTAL TECHNIQUES

Cu substituted Ni-Zn ferrites of chemical formulation $\text{Ni}_{0.2}\text{Cu}_x\text{Zn}_{0.8-x}\text{Fe}_2\text{O}_4$ were synthesized by Citrate-Gel Auto Combustion. Stoichiometric amounts of metal nitrates of nickel, copper, ferric and zinc of 99% purity are dissolved in distilled water and later mixed with citric acid in 1:1 ratio. This mixture after stirring was heated to 80°C and by adding ammonia the solution pH value was set to 7 to form a sol. The resulting solution was made to form a viscous gel on stirring and heating between 180°C - 200°C to result in ferrite powder. This ferrite powder was grinded using Agate Mortar and calcinated for four hours at 500°C . This powder was mixed with 10%

polyvinyl alcohol (PVA) and pressed to form pellets by applying pressure of 10-ton cm^{-2} . The pellets were finally sintered and coated with silver paste to provide electrical contact.

Bruker D8 X-Ray Diffractometer was used to analyze the structure and phase nature of the sintered nano-particles. XRD patterns indicated strongest reflection by peak 311 for all samples. Debye-Scherrer's formula was used to calculate the crystalline size from HWM of reflection peak 311 for all samples [14] while the experimental density was derived from Archimedes principle in xylene media. Reflection and absorption in uv region were given by UV-DRS spectroscopy. During absorption energy is absorbed by the molecules of electron in uv or visible form of light and this electron gets excited to higher orbit [15]. The band gap energy was calculated by using the formula

$$E = \frac{hc}{\lambda} \text{ (or) } E = \frac{1240}{\lambda}$$

The seebeck coefficient (S) is derived using the formula [16]

$$S = \frac{\Delta E}{\Delta T} \text{ } (\mu\text{V}/\text{K}) \text{ (1)}$$

where the thermo emf is denoted by ΔE and ΔT denote the difference of temperature between pellets surfaces.

Activation energies are derived from slopes of plot between temperature and electrical conductivity using Arrhenius relation

$$\rho = \rho_0 e^{-E_g/kT} \text{ (2)}$$

where E_g is activation energy, k the Boltzmann constant.

M_s and H_c are related through Brown's equation [17]

$$H_c = \frac{2K_1}{\mu_0 M_s} \text{ (3)}$$

in which H_c is inversely proportional to M_s and correlates with our experimental results.

III. RESULTS AND DISCUSSION

3.1. XRD analysis

XRD patterns of the prepared Cu substituted Ni-Zn ferrite sample was displayed in Figure 2. These patterns confirm single phase cubic spinel structure for (111), (220), (311), (222), (400), (422), (511) and (440) planes which matches with standard pattern JCPDS file number-48-0489.

Table 1. displays lattice parameter, crystallite size, volume and x-ray density of all samples. It is clear from Table 1 that the crystallite

size ranges between 14.7 nm to 34.5 nm. This decrease in the crystallite size is due to ionic radius of Cu^{+2} (0.73 Å) being smaller than that of Zn^{+2} (0.74 Å). Lattice parameters decrease with increased Cu concentration obeying Vegard's law [18]. X-ray density was observed to increase with increased Cu concentration since x-ray density depends on the molecular weight and lattice parameter of the sample. Volume of the unit cell also decreased since it depends on lattice parameter. It is also observed that experimental density less than X-ray density of the sample. The experimental density and lattice parameters of the prepared sample with Cu substituted compositions were shown in Figure 3

3.2. Optical Studies

Optical studies related to prepared nano-ferrites was performed taking BaSO_4 as reference with absorbance versus wavelength by using the technique of UV-DRS. During absorption, molecules of electron absorb energy in the form of UV or visible light exciting the electron to higher orbit [19]. Cu substituted Ni-Zn ferrite has wavelength 499 nm and it is a visible region.

A wavelength of 499 nm was observed for particles under study in Figure 4. Increase in Cu concentration decreases wavelength and the absorption edge shifts from 499 nm to 485 nm. In case of Cu substituted Ni-Zn ferrite for composition $x=0.2$ blue shift is observed which may be due to increase in particle size leading to expansion of band gap [20]. The synthesized samples band gap energy calculated from following question $B.E = 1240/\lambda$ [21]. The calculated band gap energy of pure $\text{Ni}_{0.2}\text{Zn}_{0.8}\text{Fe}_2\text{O}_4$ was 2.48 eV. The band gap energy is increased with increasing of dopant concentration of Cu, i.e. 2.48 to 2.55 eV, it could be due to partial size, method of synthesis and lattice parameters of the samples. The observed values of cut off wave length and band gap energy were tabulated in Table 2

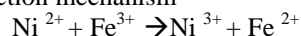
3.3. High Temperature Thermo Electric Power

The values of Seebeck Coefficient have been given Table 3. It can be seen from the table that the values of Seebeck Coefficients are positive. Depending on the sign of Seebeck coefficient current nano-ferrites under study are classified as P-type semiconductors. All composition of Ni-Zn-Cu nano-ferrites are useful in Semi conductor industry.

Thermoelectrical power for current samples has been obtained using differential method between 200°C - 600°C. In view of higher stability, the thermo emf for all samples is carried out in cooling cycle. Seebeck coefficients for these nano-

ferrites are derived from observed thermoelectric values and are tabulated in Table 3.

Table 3 indicates that Seebeck coefficients for all samples are positive indicating majority of charge carriers to be holes. The existence of Ni on B-sites favors conduction mechanism



This is due to copper ions occupying B-sites and transferring Fe^{3+} ions to A-site thereby decreasing Fe^{3+} ions in B-site with increasing Cu concentration.

Seebeck coefficient (S) for cubic spinel systems is given by

S = Total number of Fe^{3+} ions on B-sites / Total number of Fe^{2+} ions on B-sites

Increase in Cu concentration decreases the number of Fe^{2+} ions on B-sites increasing the Seebeck coefficient in Ni-Zn ferrites as per the definition of S above. The variation of Seebeck Coefficient (S) with temperature for all samples was shown in Figure 5 which indicated positive value between low to high temperature but for pure Ni-Zn ferrite it is negative to positive with increasing temperature. S was positive value for all ferrite samples under study. These samples exhibit the characteristics of p-type semiconductor in high temperature region excepting pure Ni-Zn ferrites. Pure samples at low temperatures behave like n-type semiconductor. With increase in temperature, it behaves like p-type semiconductor due to predominant conduction mechanism. Figure 5 indicates measurements of thermoelectric power carried out between 200°C–600°C using differential method. Thermoelectric power exhibits a clear transition at Curie temperature just like magnetic properties. Minimum value of Seebeck coefficient at T_c indicates the influence of magnetic ordering on thermoelectric power of current samples under investigation [22].

3.4. High Temperature Electrical conductivity

The electrical conductivity of the prepared nano-ferrite samples from under room temperature to 530°C was reported. It reduces with enhanced temperature for every sample indicating semiconducting nature. Figure 6 shows the plot of $\text{Log}(\sigma T)$ vs $1000/T$ indicating a curve from which samples thermal activation energy can be derived from slope. As per the plot electrical conductivity of Cu substituted Ni-Zn nano ferrites show discontinuity having two different regions with variation in activation energies resulting in paramagnetic and ferrimagnetic regions. As per

magnetic semiconductor theory, ferrimagnetic and paramagnetic represent ordered and disordered regions [23]. Hence extra energy is required for conduction in paramagnetic region than ferrimagnetic region. Hence, the activation energy in the paramagnetic region (EP) is found greater than the ferrimagnetic region (EF). Similar results were reported by others in Zn-Ni ferrites [24]. The activation energy values in the paramagnetic region and ferromagnetic region with Curie temperature values are tabulated in Table 4.

IV. CONCLUSIONS:

XRD pattern for investigative samples confirmed single phase cubic spinel structure.

Doping copper in Ni-Zn ferrite system decreases lattice parameter and increases x-ray density.

Crystallite size of the sample ranges between 14.7 nm–34.5 nm.

Optical studies by UV–DRS decrease in wavelength with increase in Cu concentration. The absorption edge shifts from 499 nm to 485 nm.

Thermoelectric power measurements are taken up in the range of 200°C–600°C using differential method.

Seebeck coefficient attained positive value for all ferrite samples under study. This indicated p-type semiconducting nature in high temperature region for prepared samples with exception of pure Ni-Zn ferrites.

Depending on the sign of Seebeck coefficient current nano-ferrites under study are classified as P-type semiconductors. All composition of Ni-Zn-Cu nano-ferrites are useful in Semiconductor industry.

Electrical conductivity of the prepared sample between room temperature to 530°C clearly indicated decrease in electrical conductivity with increase in temperature for all samples indicating semiconducting nature of the prepared ferrite samples resulting to para and ferrimagnetic regions.

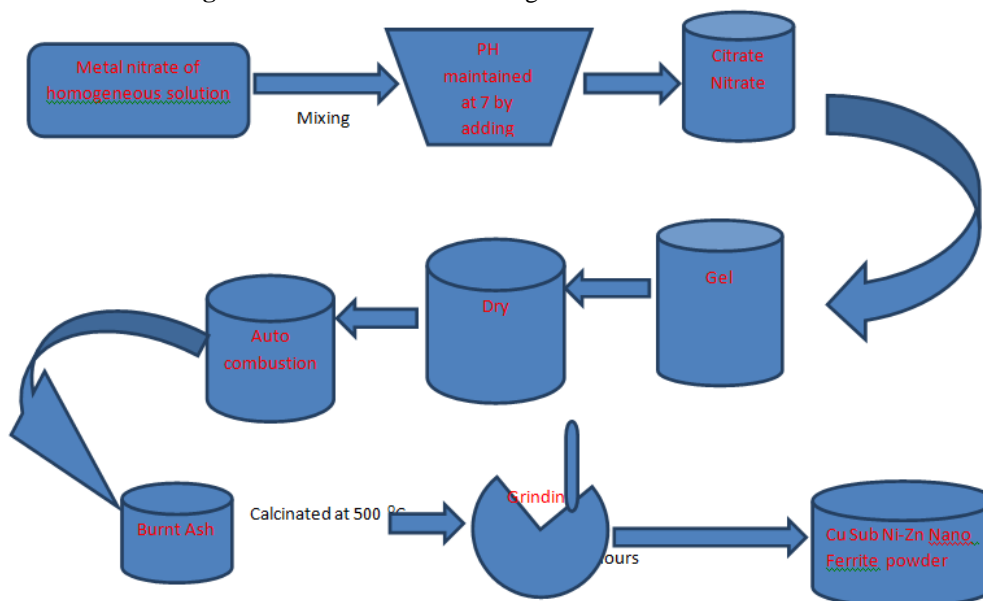
Acknowledgements: The authors are very grateful to Prof. D. Karuna Sagar, Head, and Prof. M. Srinivas, Chairman, BOS Department of Physics, Osmania University, Hyderabad. The authors are also very grateful to Dr. Shekar Matta, Principal, Dr. B. R. Ambedkar College, Baghlingampally, Hyderabad and J. S. Harinakshi, Vice Principal, Dr. B. R. Ambedkar College, Baghlingampally, Hyderabad for their encouragement in the present Research work.

REFERENCES

- [1]. Abbas. T, Khan. Y, Ahmed. M, Anwer 1992
Solid state communi **82** 701
- [2]. Roy. P. K and Bera. J 2006 J
Magn Mater **298** 38

- [3]. Thang.P.D,Riginders.Gand.Blank.D.H 2005. J Magn Magn mater **296** 251
- [4]. Ielisei.M.F.F, Porto.A.O, goncalves.C.M and Fabris.J.D 2004 J Magn Magn mater **278**, 263
- [5]. Kumar .M.K, Singh.P.K, Kishan.P, kumar.N, Rao S.L.N, Singh.P.K, and Srivathsava.S.L 1998 J Appli Physics, **63** 3780
- [6]. Dias.A, and Moreira.R.L 1999 Mat Letters **39** 69
- [7]. Jacobo.S.E, Duhalde.S and Bertorello.H.R.2004. J of Mag and Mag Matrels Vol **272** 2253
- [8]. Shenoy.S.D,Joy.P.A and Anantharaman.M.R,2004 J of Magn Magn mater **269** 2217.
- [9]. Morrison.S.A, Cahill.C.L, Carpenter.E.E,E.Calvin.S, Swaminathan.R.,McHenry.M.E and Harris VG 2004 J of Applied physics, **195**6392.
- [10]. Sun.J, Li.J, Sun.G and Qu.W, vol 2002 **28**,855.
- [11]. Verma.A,Goel.T.C,Mendiratta.R.G and Alam.M.I, Materials science and Engg.B 1999 **60**156.
- [12]. Lopez.G.P, Psilvetti.S, Urreta.S.E and Cabanillas.E.D,2007. Physics B, Vol **398**241.
- [13]. Upadhy.C, Mishra.D, Verma.H.C, Anand.S and Das.R.P 2003 J of mag Mag mater **260**,188.
- [14]. Suryawanshi .SS , Deshpand.V ,Sawant.SR 1999 J Mater Chem Phy **59** 199.
- [15]. Cumbale.R.C, Sheikah.P.A, camble .S.S and Kolekar .Y.D 2009 J Alloys and Compounds **478** 599.
- [16]. Raghassudha.M, Ravinder.D,Veerassomaiah.P,2014. J. Alloys Comp. **604**, 276
- [17]. Coey.J.M.D, John Wiley and Sons,1996 New York, .
- [18]. Singh,S.C, Jauhar, Kumar.V, Singh.J, Singha.S 2015 Mat. Chem. Phys. **156**, 188.
- [19]. Pan.L.K, Sun.C.Q, Tay.B.K, Chen.T.P,2002 Phys.Chem.B **106** 11725.
- [20]. Suryawanshi SS, Deshpand.V,Sawant.SR 1999. J Mater Chem Phy **59** 199.
- [21]. Ravi Kumar.D, Abraham Lincoln.Ch, Ravinder.D, Syed Ismail Ahmad Applied physics A (IF 1.810) Pub Date: **2020-08-17**, DOI: 10.1007/s00339-020-03894-8
- [22]. Aravind.G ,Raghassudha.M ,Ravinder.D , Abdul Gaffoor And Nathaniel.V 2015. J NanostructChem **5** 77.
- [23]. Sridhar.R, Ravinder.D, Kumar.K.V 2012. Advances in Materials Physics and Chemistry **2**, 192
- [24]. Shabasy-EI,1999 Journal of Magnetism and Magnetic Materials **172**, 188.

Figure 1. Flow Chart for Citrate gel auto combustion method



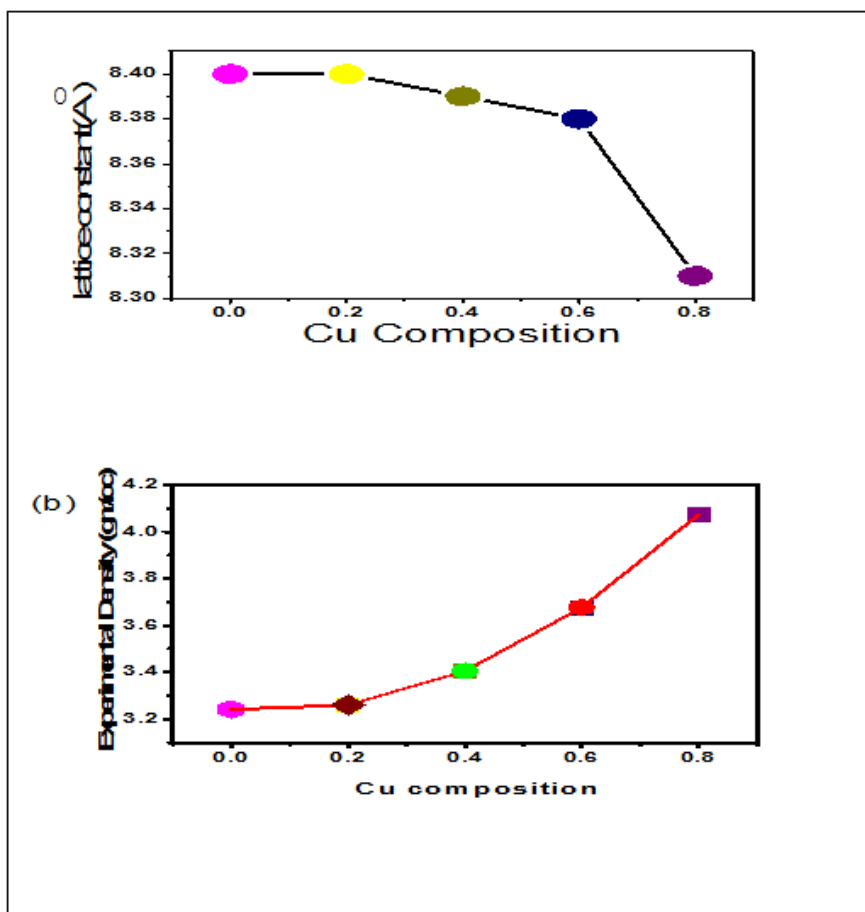
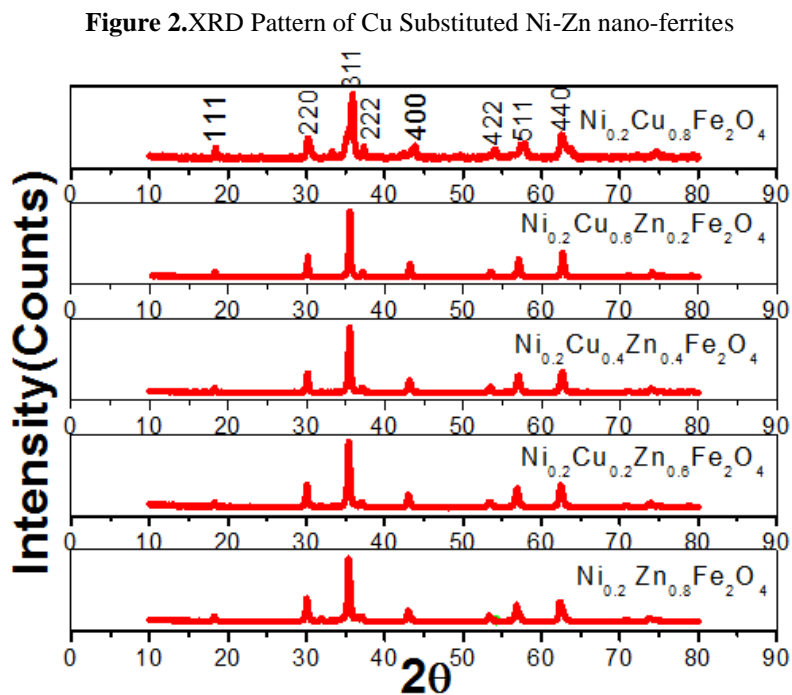


Figure 3. Variation of (a) Lattice parameter and (b) Experimental density with composition of Ni_{0.2}Cu_xZn_{0.8-x}Fe₂O₄ nano ferrites.

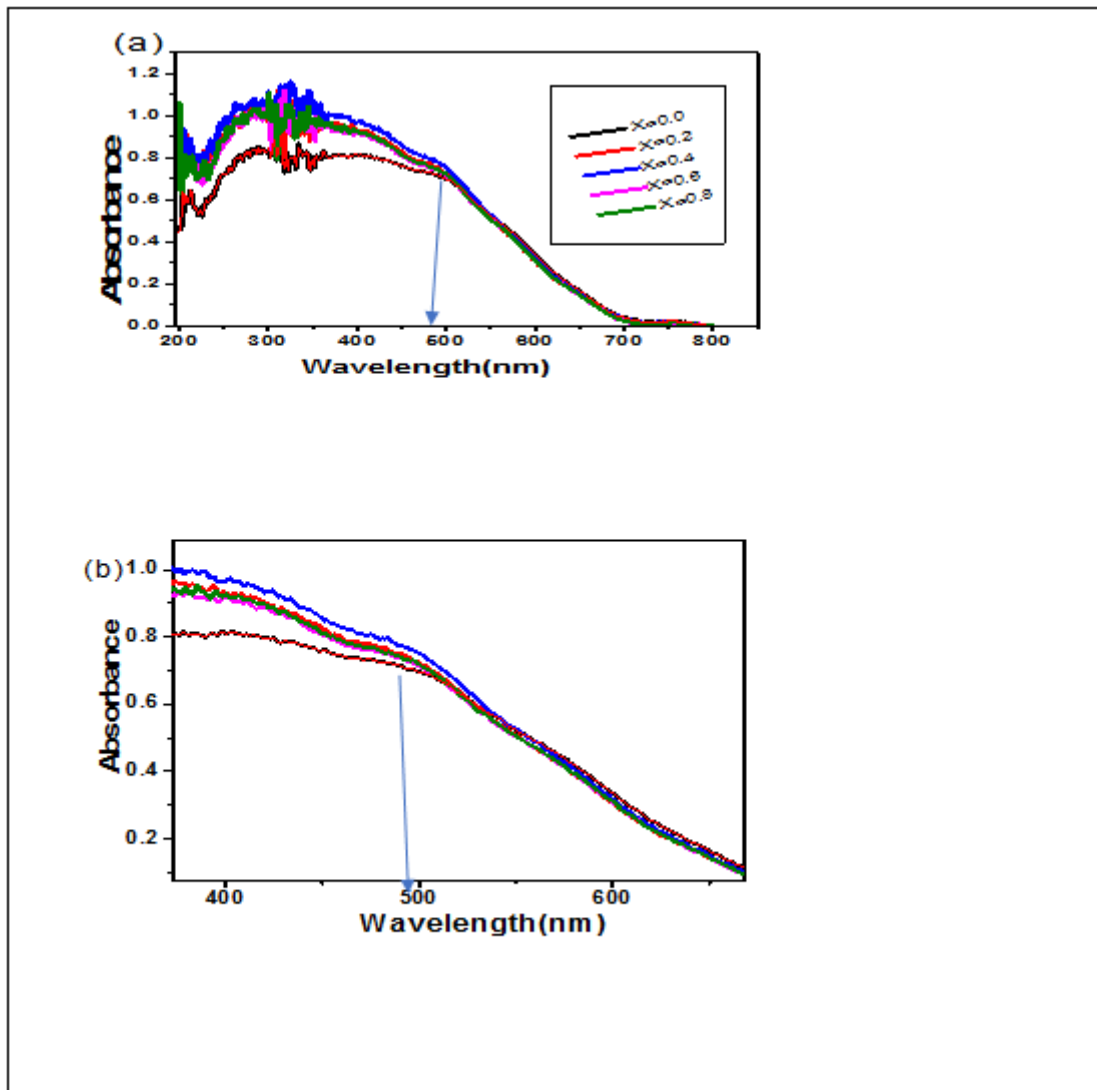
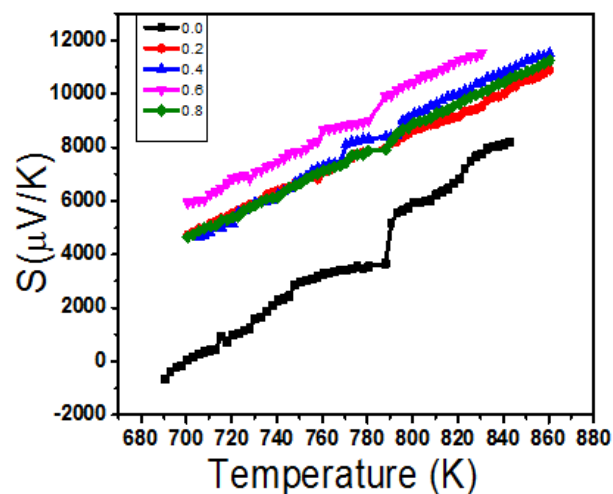
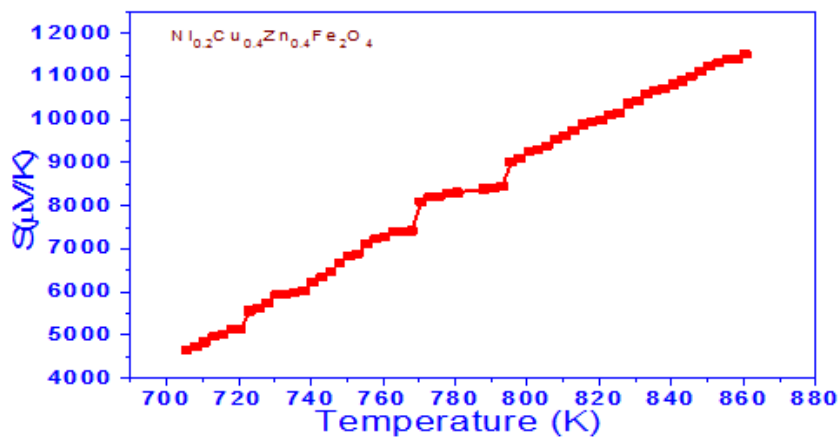
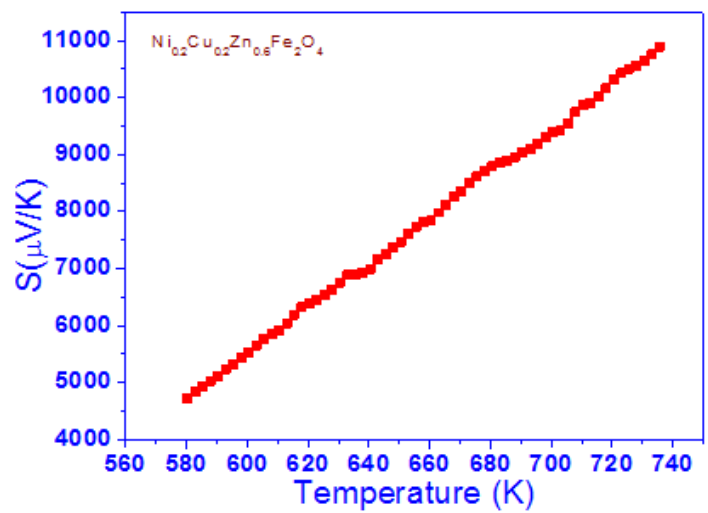
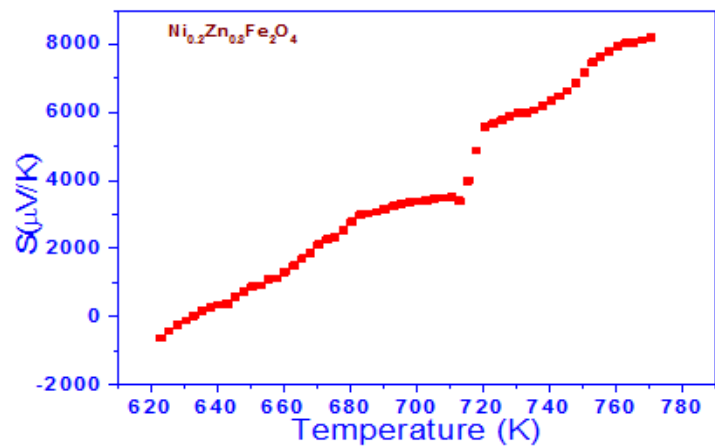


Figure 4(a-b). UV-visible spectra of nano-crystalline $\text{Ni}_{0.2}\text{Cu}_x\text{Zn}_{0.8-x}\text{Fe}_2\text{O}_4$

Figure 5. Dependence of Seebeck Coefficient on Temperature for Cu substituted Ni-Zn nanoferrites





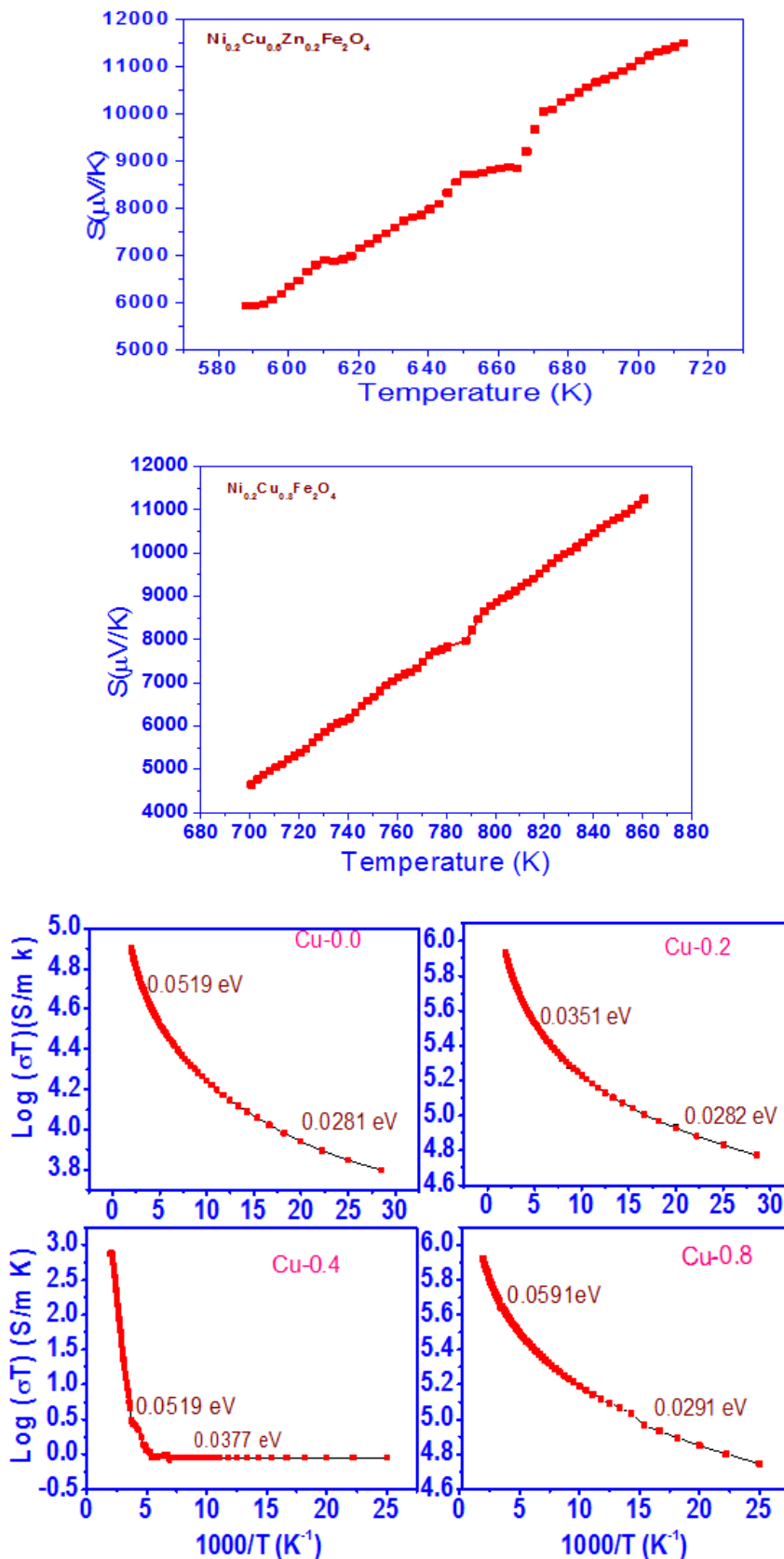


Figure 6 Temperature variation of Electrical conductivity of $\text{Ni}_{0.2}\text{Cu}_x\text{Zn}_{0.8-x}\text{Fe}_2\text{O}_4$ nano ferrites.

Table1. Structural parameters of the prepared Cu substituted Ni-Zn nano ferrite sample

S.no	Composition	Mol.Wt(g m/mol)	Crystallite size(nm)	Lattice constant (A°)	X-ray density(d_x) (gm/cc)	Volume (A°) ³	Ex. density(d_e) (gm/cc)
1	Ni _{0.2} Zn _{0.8} Fe ₂ O ₄	239.73	22.7	8.40	5.35	594.2	3.2
2	Ni _{0.2} Cu _{0.2} Zn _{0.6} Fe ₂ O ₄	239.36	25.2	8.40	5.36	594.07	3.3
3	Ni _{0.2} Cu _{0.4} Zn _{0.4} Fe ₂ O ₄	239	24.1	8.39	5.38	589.8	3.4
4	Ni _{0.2} Cu _{0.6} Zn _{0.2} Fe ₂ O ₄	238.63	34.5	8.38	5.39	588.2	3.6
5	Ni _{0.2} Cu _{0.8} Fe ₂ O ₄	238.26	14.7	8.31	5.50	574.5	4.1

Table 2. Ni_{0.2}Cu_xZn_{0.8-x}Fe₂O₄ nano ferrites Cut off wave length with Band gap energy

Composition	Cut off wave length	Band gap energy
Ni _{0.2} Zn _{0.8} Fe ₂ O ₄	499	2.484
Ni _{0.2} Cu _{0.2} Zn _{0.6} Fe ₂ O ₄	485	2.556
Ni _{0.2} Cu _{0.4} Zn _{0.4} Fe ₂ O ₄	489	2.535
Ni _{0.2} Cu _{0.6} Zn _{0.2} Fe ₂ O ₄	487	2.546
Ni _{0.2} Cu _{0.8} Fe ₂ O ₄	486	2.551

Table 3. Seebeck Coefficient and Curie temperature of Ni_{0.2}Cu_xZn_{0.8-x}Fe₂O₄

S.no	Composition	Curie Temperature (K)	Seebeck Coefficient (s)($\mu V/K$) at 730K
1	Ni _{0.2} Zn _{0.8} Fe ₂ O ₄	789	+1600
2	Ni _{0.2} Cu _{0.2} Zn _{0.6} Fe ₂ O ₄	780	+ 5910
3	Ni _{0.2} Cu _{0.4} Zn _{0.4} Fe ₂ O ₄	765	+ 5930
4	Ni _{0.2} Cu _{0.6} Zn _{0.2} Fe ₂ O ₄	779	+ 7070
5	Ni _{0.2} Cu _{0.8} Fe ₂ O ₄	781	+ 5830

Table4. Activation energies of Ni_{0.2}Cu_xZn_{0.8-x}Fe₂O₄ nano-ferrites with Curie Temperatures

S.No	composition	Curie Temp (°C)	Para Region (E _p) eV	Ferri Region (E _F) eV
1	Ni _{0.2} Zn _{0.8} Fe ₂ O ₄	516	0.052	0.028
2	Ni _{0.2} Cu _{0.2} Zn _{0.6} Fe ₂ O ₄	507	0.035	0.028
3	Ni _{0.2} Cu _{0.4} Zn _{0.4} Fe ₂ O ₄	492	0.052	0.038
4	Ni _{0.2} Cu _{0.8} Fe ₂ O ₄	508	0.059	0.029